3. Single gravestone or group of gravestones, and
4. Gravestone removed, so that sample was exposed only by scattering from wet soil or granite surface, not the gravestone itself.

The gravestone results are used for the intercomparison samples and other samples where the exact geometry is unknown.

In Table B3, TFs are calculated in a core of the Saikoji gravestone for all the measured activations.

In Table B4, the cores from City Hall were recalculated with two variations:

1. City Hall cores exposed to DS86 free-field fluences
2. City Hall cores without the trace neutron poisons exposed to DS02 free-field fluences

While the DS86 spectrum, compared to DS02, has slightly more neutron fluence with energies greater than 3 MeV, the TFs calculated with the DS86 spectra are essentially the same as from DS02 at all depths. Removing the trace poisons causes a small increase (+1%) on the surface of the City Hall concrete. At depth, the TF goes up about +20 to +30%.

In Table B5, various activations are calculated at the cobalt sample locations.

In Tables B6 through B9, the TF, the calculated ^{36}Cl activation, and the FIA equivalent ^{36}Cl activation at a height of 1 m above ground for every ^{36}Cl sample are given for Nagashima, Rühm, Straume granite, and Straume concrete samples, respectively. The columns in the table are as follows:

1. Sample identification (if any)
2. Note is made if it is an intercomparison sample.
3. Location
4. Mean depth (MD) in cm
5. Originally reported ground range in meters
6. DS86 hypocenter ground range in meters
7. DS02 hypocenter ground range in meters
8. Slant range (SR) in meters
9. Sample height (Ht) in meters
10. Net measurement (Net meas) of the ^{36}Cl-measured activation in units of atoms of ^{36}Cl per atoms of Cl at the time of bombing. Background has been subtracted.
11. Investigator's reported measurement error (or estimated standard deviation [SD] for the measurement). This will be used to weight measurements when determining goodness of fit to the calculations. A minimum uncertainty of 3% is used in the comparisons to calculations (Chapter 12, Part D).
12. K atoms per Cl atom (K/Cl) in sample. If not known, then 300 ppm is assumed.

13-15. Calculated FIA activation for ^{36}Cl from ^{39}K and ^{35}Cl, and for ^{152}Eu from ^{151}Eu with same units as given in tables of Chapter 3 (^{36}Cl per K atom, ^{36}Cl per Cl atom, Bq of ^{152}Eu per mg of Eu).

16. Brief description of shielding model used to obtain the TF.

17-19. Calculated TF for ^{39}K, ^{35}Cl, and ^{151}Eu reactions using DS02 Hiroshima fluences.

20-22. Calculated *in situ* ^{36}Cl activation from ^{35}Cl(n,γ)^{36}Cl and ^{39}K(n,α)^{36}Cl reactions. The total ^{36}Cl activation is also given.

23. Free-in-air equivalent ^{36}Cl measured activation at 1 m above ground derived from ^{36}Cl *in situ* measurement. This is obtained by subtracting the ^{39}K(n,α)^{36}Cl calculated

activation from the measured ^{36}Cl and then dividing by the transmission factor for $^{35}Cl(n,\gamma)^{36}Cl$, TF_{Cl}, as shown in the formula:

$$Meas_{FIA\ ^{36}Cl} = (Meas_{in\ situ\ ^{36}Cl} - N_K/N_{Cl} * FF_K * TF_K) \ / \ TF_{Cl}$$

The free-in-air equivalent ^{36}Cl measured activation data can be compared directly with a smooth curve of the 1 m above ground ^{36}Cl activation. The smooth curve is not dependent on information about the amount of potassium, K, in the sample. While this approach is very convenient for comparing Cl measurements with the DS02 Cl calculations and to non-chlorine measurements, it must be remembered that the FIA equivalent measurement will be slightly affected by uncertainty of the fast fluence, K/Cl ratio and K thermal neutron cross section.

In Table B10, the TF, the calculated ^{36}Cl activation, and the FIA equivalent ^{36}Cl measured activation at a height of 1 m above ground for Shizuma et al. ^{152}Eu measurements from four cores are given (Shizuma et al. 1997, Chapter 8, Part C). The table has many of the same columns as did the previous table. The new columns are described as follows:

10. ^{152}Eu measurement in units of Bq mg^{-1} at time of bombing
20. *In situ* ^{36}Cl calculated activation from $^{35}Cl(n,\gamma)^{36}Cl$
21. *In situ* equivalent ^{36}Cl measured activation. This is obtained by converting the ^{152}Eu measured activation into ^{36}Cl by multiplying by the free-field calculated activation ratio and the TF ratio between $^{35}Cl(n,\gamma)^{36}Cl$ and $^{151}Eu(n,\gamma)^{152}Eu$ activation as shown in the formula:

$$Meas_{in\ situ\ ^{36}Cl} = (Meas_{in\ situ\ ^{152}Eu} * FF_{Cl} / FF_{Eu} * TF_{Cl} / TF_{Eu})$$

The *in situ* equivalent ^{36}Cl measured activation from ^{152}Eu measurements can be compared directly with *in situ* ^{36}Cl measured activation, and with *in situ* ^{36}Cl DS02 activation, which is a smooth curve as a function of depth.

In Table B11, the TF, the calculated ^{36}Cl activation, and the FIA equivalent ^{36}Cl activation at a height of 1 m above ground for Komura's intercomparison europium core measurements (Chapter 8, Part I) are given. The table has the same columns as the previous table.

Calculations of TFs for the ^{60}Co measurements in iron rebar in Hiroshima (Chapter 8, Part A) and the ^{36}Cl measurements in concrete cores in Nagasaki (Chapter 8, Part D) were performed and are used for comparing those measurements to DS02. TFs for the Nagasaki Cl core samples are given in Table B12. In Table B13, the TFs, the calculated ^{36}Cl activation, and the FIA equivalent ^{36}Cl activation at a height of 1 m above ground for the Nagasaki core samples are given.

Default Thermal Neutron Transmission Factors and Uncertainty

The complete set of TFs was examined for information about default TFs for samples that are not well defined and to estimate uncertainty for all TFs. Figure 2 shows all of the ^{36}Cl TFs that were calculated. They are plotted against depth to distribute them. Three of the core calculations are highlighted by a connecting curve. The City Hall core, which is typical of concrete, is plotted as a solid green line. The TFs start at 1.05 on the surface, build up to 1.10 at 5 cm and then fall off an order of magnitude ~35 cm afterward. The original granite core of Shirakami Shrine is shown as a blue dash. There is no buildup at the surface, and the activation drops an order of magnitude in ~60 cm. With a wood cover over the Shirakami granite rock, shown as a red dot, the surface activation increases by more than 50% at the surface. But then the activation drops an

order of magnitude in ~40 cm.

The TFs for surface samples range from 0.6 to 1.1. They can be assigned to TF categories based on the materials they are found in and the type of ground it is exposed to:

Concrete sample surface exposed to soil:	TF = 1.05 at surface, 1.10 at 5 cm
Concrete sample surface exposed to concrete:	TF = 1.0 at surface, 1.10 at 5 cm
Concrete sample surface exposed to granite:	TF = 0.9 at surface, 1.10 at 5 cm
Granite sample surface exposed to soil:	TF = 0.9 at surface, 0.80 at 5 cm
Granite sample surface not line-of-sight to soil:	TF = 0.8 at surface, 0.75 at 5 cm
Granite sample surface exposed to concrete:	TF = 0.8 at surface, 0.75 at 5 cm
Granite sample surface exposed to granite:	TF = 0.7 at surface, 0.65 at 5 cm

From the range of TFs that has been calculated, a typical TF for Cl and Eu is about 1.1 in concrete and 0.85 in granite. The typical TF for Co is about 0-5% larger.

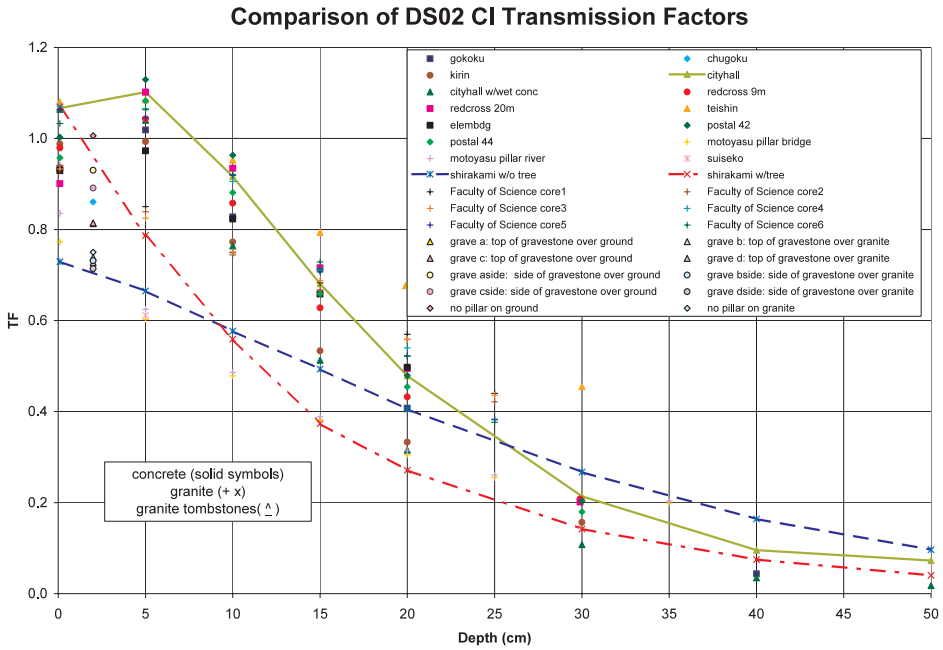

Figure 2. *All calculated transmission factors as a function of depth into concrete and granite samples. Three cores are illustrated with curves;*

1) City Hall concrete core,

2) Shirakami granite rock, and

3) Shirakami granite rock with wood covering.

Except for the Motoyasu bridge railing, the intercomparison samples did not have geometry descriptions detailed enough to do sample-specific TF calculations. These other samples were all of granite material. Gravestone “c” was chosen to represent the TF for these samples. Gravestone “c” is located 2 cm from the top surface of the gravestone with a few nearby gravestones all on

top of Hiroshima wet soil. The TF for this calculation is about 0.83. For granite samples, the range of the TF includes having the sample in an all granite environment (TF = 0.72) or under foliage (TF = 0.95). Both of those are limiting events. If it is assumed that this represents two standard deviations, then one standard deviation for the calculated TFs is about 7% for the intercomparison samples.

For non-intercomparison samples, when the material is known to be granite or concrete with a clear line-of-sight to the epicenter, then a TF uncertainty of 7% is reasonable. If the sample material is unknown but the geometry has clear line-of-sight to the epicenter, then 15% is reasonable.

References

Fujita, S. Personal Communications to T. Straume and others with drawings, photographs, and descriptions of samples locations at Hiroshima and Nagasaki, 1990-2002.

Galbraith Laboratories, Inc. Personal Communications in the form of Laboratory Reports to T. Straume, 2000-2001.

Hasai, H.; Iwatani, K.; Shizuma, K.; Hoshi, M.; Yokoro, K.; Sawada, S.; Kosako, T.; Morishima, Y. "^{152}Eu Depth Profile of Stone Bridge Pillar Exposed to the Hiroshima Atomic Bomb." In: *US-Japan Joint Reassessment of Atomic Bomb Radiation Dosimetry in Hiroshima and Nagasaki, Final Report, Vol. 2*, pp. 295-309 (Roesch, W. C.; ed.). Hiroshima, Japan: Radiation Effects Research Foundation; 1987.

Hiroshima Peace Memorial Museum. *Architectural Witness to the Atomic Bombing—A Record for the Future* (in Japanese). Hiroshima, Japan: Hiroshima Peace Memorial Museum; 1996.

Ingersoll, D. T.; Roussin, R. W.; Fu, C. Y.; White, J. E. *DABL69: A Broad-Group Neutron/Photon Cross-Section Library for Defense Nuclear Applications.* Oak Ridge, Tennessee: Oak Ridge National Laboratory; ORNL/TM-10568; 1989.

Ingersoll, D. T.; White, J. E.; Wright, R. Q.; Hunter, H. T.; Slater, C. O.; Greene, N. M.; Roussin, R. W.; MacFarland, R. E. *Production and Testing of the VITAMIN-B6 Fine Group and BUGLE-93 Broad Group Neutron/Photon Cross-Section Libraries Derived from ENDF/B-VI Nuclear Data.* Washington, D.C.: U.S. Nuclear Regulatory Commission, NUREG/CR-6214 (ORNL-6214); 1995.

Johnson, J. O.; ed. *A User's Manual for MASH 1.0—A Monte Carlo Adjoint Shielding Code System.* Oak Ridge, Tennessee: Oak Ridge National Laboratory; ORNL/TM-11778; 1999.

Kerr, G. D. *Neutron Activation of Surface-Iron Samples from Hiroshima*. Oak Ridge National Laboratory, Memorandum to J. V. Pace III, Oak Ridge National Laboratory; Oak Ridge, Tennessee; 1985.

Kerr, G. D.; Pace, J. V. III; Mendelsohn, E.; Loewe, W. E.; Kaul, D. C.; Dolatshahi, F.; Egbert, S. D.; Scott, W. W. Jr.; Marcu, J.; Kosako, T.; Kanda, K. "Transport of Initial Radiations in Air Over Ground." In: *US-Japan Joint Reassessment of Atomic Bomb Radiation Dosimetry in Hiroshima and Nagasaki, Final Report, Vol. 1*, pp. 66-142 (Roesch, W. C.; ed.). Hiroshima, Japan: Radiation Effects Research Foundation; 1987.

Kerr, G. D.; Dyer, F. F.; Emery, J. F.; Pace, J. V. III; Brodzinski, R. L.; Marcum, J. *Activation of Cobalt by Neutrons from the Hiroshima Bomb.* Oak Ridge, Tennessee: Oak Ridge National Laboratory; ORNL-6590; 1990.

Krauthan, P. Diploma Thesis, Technical University of Munich, 1988 (in German)

Maruyama, T.; Kawamura, K. "Comments on ^{60}Co Measurements." In: *US-Japan Joint Reassessment of Atomic Bomb Radiation Dosimetry in Hiroshima and Nagasaki, Final Report, Vol. 2,* pp. 335-339 (Roesch, W. C.; ed.). Hiroshima, Japan: Radiation Effects Research Foundation; 1987.

McVane, V.; Dunford, C. L.; Pose, P. F.; eds. *ENDF-102: Data Formats and Procedures for the Evaluated Nuclear Data File ENDF-6.* Upton, New York: Brookhaven National Laboratory; BNL-NCS-44945 Revised; 1995.

Mughabghab, S. F.; Divadeen, M.; Holden, N. E. *Neutron Cross Sections, Vol. 1 Neutron Resonance Parameters and Thermal Cross Sections, Part A, Z=1-60.* Upton, New York: Brookhaven National Laboratory; National Nuclear Data Center; Academic Press; 1981.

Mughabghab, S. F.; Divadeen, M.; Holden, N. E. *Neutron Cross Sections, Vol. 1 Neutron Resonance Parameters and Thermal Cross Sections, Part B, Z=61-100.* Upton, New York: Brookhaven National Laboratory; National Nuclear Data Center; Academic Press; 1984.

Nakanishi, T.; Kobayashi, K.; Yamamoto, T.; Miyaji, K. "Residual Neutron-Induced Radioactivities in Samples Exposed in Hiroshima." In: *US-Japan Joint Reassessment of Atomic Bomb Radiation Dosimetry in Hiroshima and Nagasaki, Final Report, Vol. 2,* pp. 310-319 (Roesch, W. C.; ed.). Hiroshima, Japan: Radiation Effects Research Foundation; 1987.

Rühm, W. *Das Neutronenspektrum von Hiroshima und das Dosimetriesystem DS86.* Munich, Germany: Technical University of Munich, PhD Thesis; 1993 (in German).

Rühm, W.; Huber, T.; Kato, K.; Nolte, E. *Measurement of ^{36}Cl at Munich—A Status Report*. Radiobiological Institute, Ludwig Maximilians University of Munich: Technical Report SBI 212/11.2000; 2000.

Shibata, K.; Nakagawa, T.; Asami, T.; Fukahori, T.; Narita, T.; Chiba, S.; Mizumoto, M.; Hasegawa, A.; Kikuchi, Y.; Nakajima, Y.; Igarasi, S. *Japanese Evaluated Nuclear Data Library, Version-3- JENDL-3.* Tokai-mura, Naka-gun, Ibaraki-ken, Japan: Japan Atomic Research Institute; JAERI 1319; 1990.

Shizuma, K.; Iwatani, K.; Hasai, H.; Hoshi, M.; Oka, T. "^{152}Eu Depth Profiles in Granite and Concrete Cores Exposed to the Hiroshima Atomic Bomb." *Health Phys.* 72: 848-855; 1997.

United States Strategic Bombing Survey (USSBS). *The Effects of the Atomic Bomb on Hiroshima, Japan.* Washington, D.C.: U.S. Government Printing Office; Vols. 1-3; 1947.

Weast, R. C.; ed. *Handbook of Chemistry and Physics.* Cleveland, Ohio: CRC Press; 56th Edition; 1976.

White, J. E.; Ingersoll, D. T.; Wright, R. Q.; Hunter, H. T.; Slater, C. O.; Greene, M. N.; MacFarlane, R. E.; Roussin, R. W. *Production and Testing of the Revised VITAMIN-B Fine-Group and the BUGLE-96 Broad-Group Neutron/Photon Cross-Section Libraries Derived from ENDF/B-VI.3 Nuclear Data.* Oak Ridge, Tennessee: Oak Ridge National Laboratory; ORNL/TM-6795/R1; April 2000.

Appendix A

Thermal Neutron Transmission Factor Shielding Models

Figures of the shielding models, which are used for thermal neutron transmission factor calculations, are found in Figures A1 through A33. In each figure, information about the sample site name, materials, local geometry coordinate system, sample calculation coordinates, and depths appear. A red star notes the calculation location. A red arrow notes the direction from the epicenter. A black arrow notes the direction to the hypocenter. The building orientation, with respect to the hypocenter, is noted by angles in degrees. Units of length are in centimeters unless otherwise indicated. The original reported ground range distances are given in meters. The TFs are calculated at this distance. More recent changes in sample ground ranges are small relative to the overall distance, and will result in very minor differences in TF (~1%).

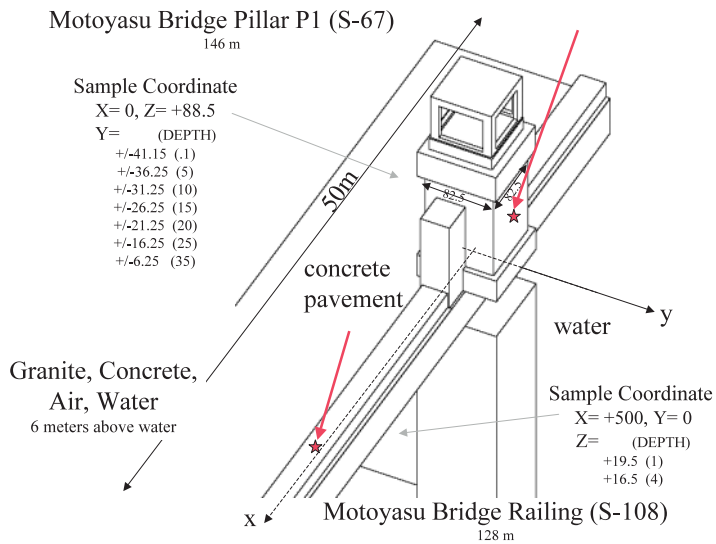

Figure A1. *Motoyasu Bridge Pillar and Railing (distances to hypocenter as originally reported)—X,Y,Z is sample location (cm) from building origin.*

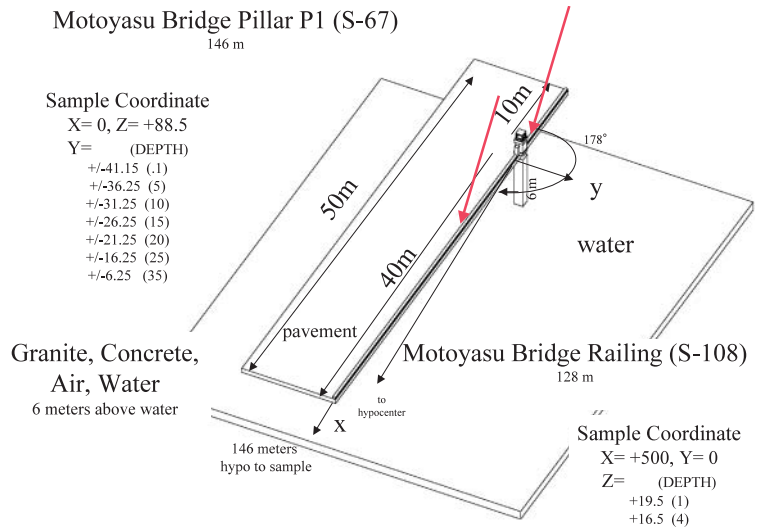

Figure A2. *Motoyasu Bridge Pillar and Railing (distances to hypocenter as originally reported)—X,Y,Z is sample location (cm) from building origin.*

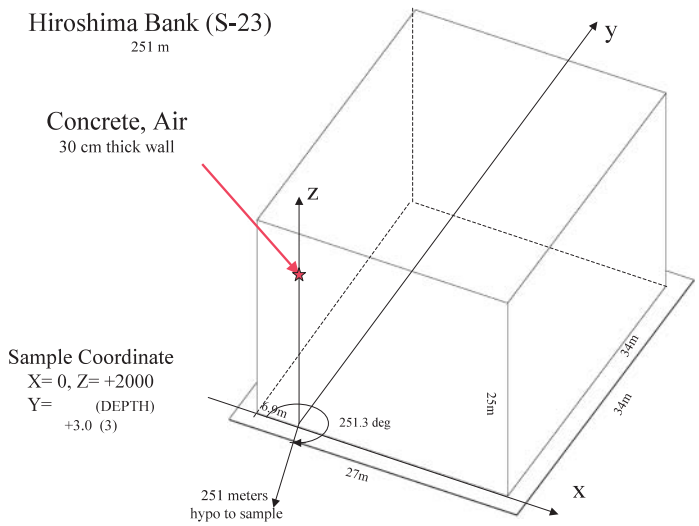

Figure A3. *Hiroshima Bank (distances to hypocenter as originally reported)—X,Y,Z is sample location (cm) from building origin.*

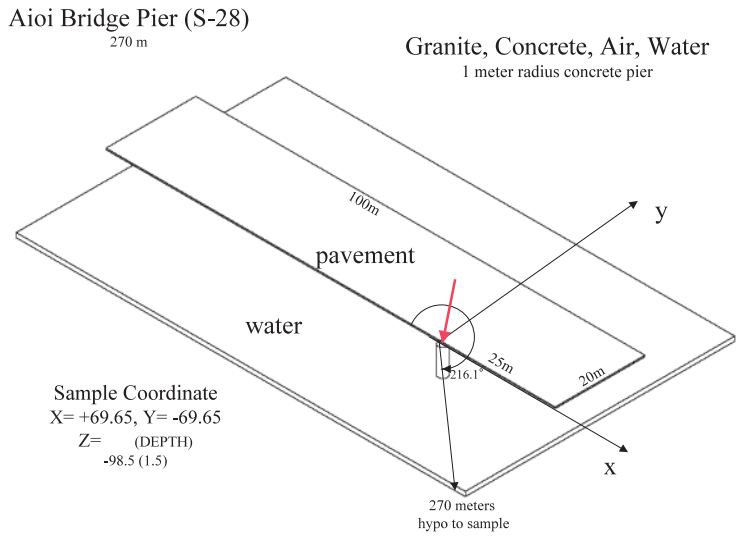

Figure A4. *Aioi Bridge Pier (distances to hypocenter as originally reported)—X,Y,Z is sample location (cm) from building origin.*

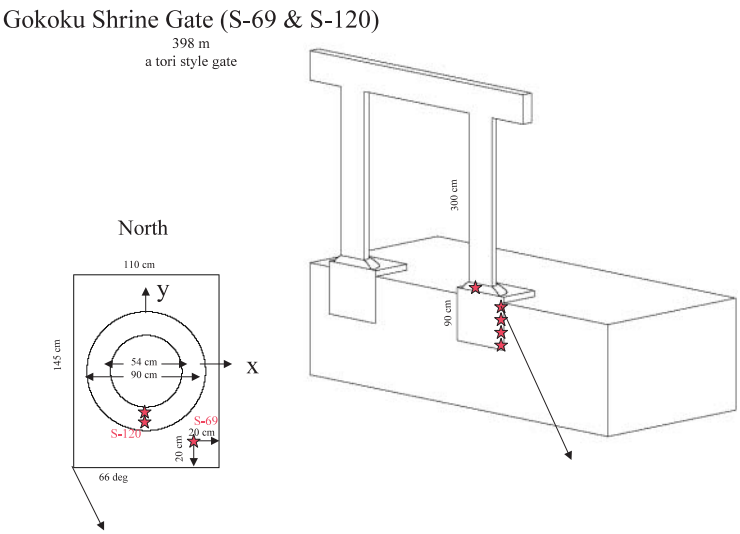

Figure A5. *Gokoku Shrine Gate Base.*

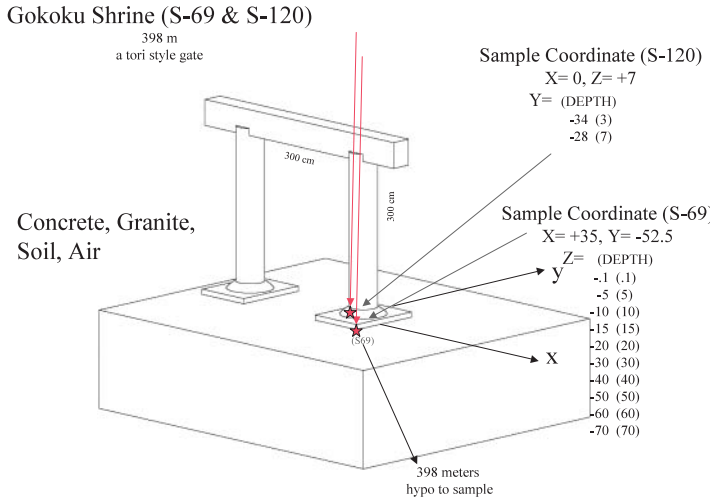

Figure A6. *Gokoku Shrine Gate Base (distances to hypocenter as originally reported)—X,Y,Z is sample location (cm) from building origin.*

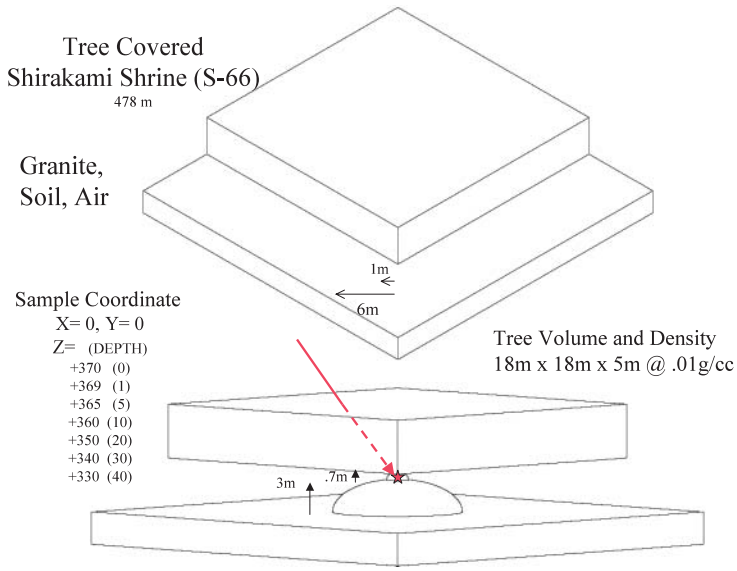

Figure A7. *Shirakami Shrine Rock covered by tree foliage (distances to hypocenter as originally reported)—X,Y,Z is sample location (cm) from building origin.*

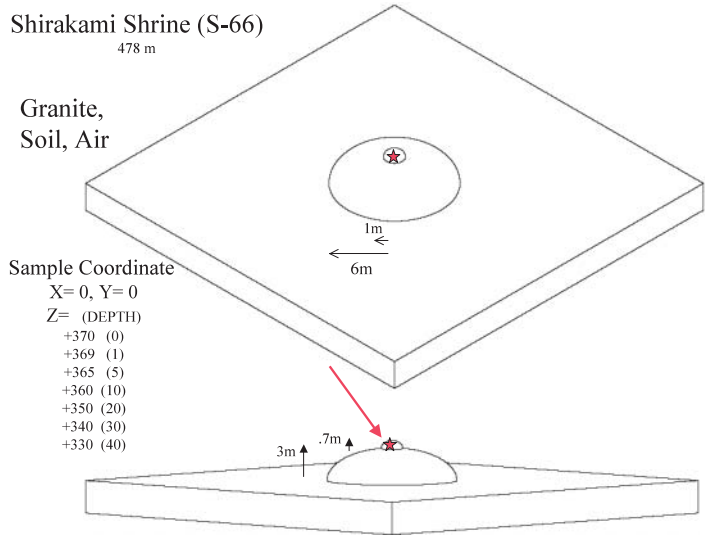

Figure A8. *Shirakami Shrine Rock not covered by tree foliage (distances to hypocenter as originally reported)—X,Y,Z is sample location (cm) from building origin.*

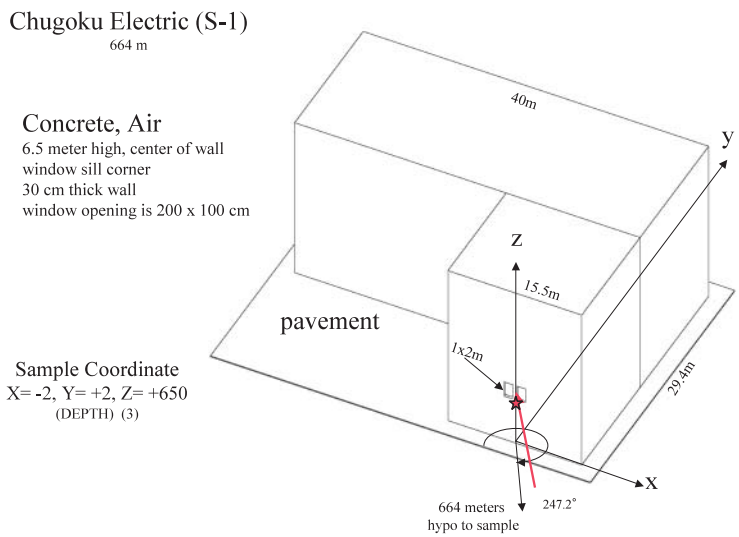

Figure A9. *Chugoku Electric Building (distances to hypocenter as originally reported)—X,Y,Z is sample location (cm) from building origin.*

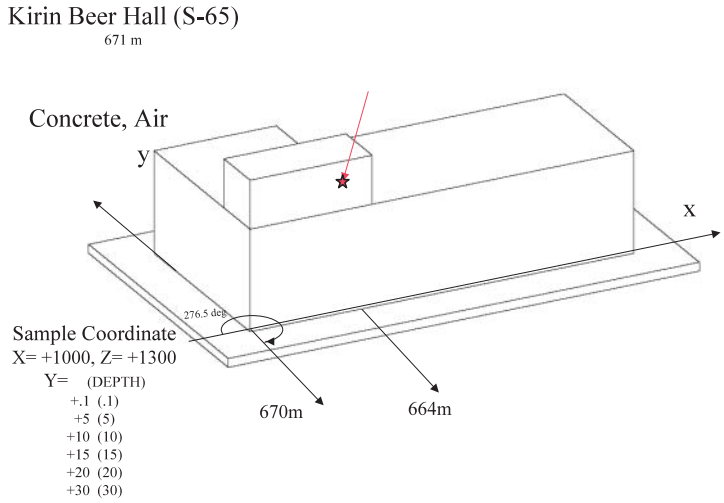

Figure A10. *Kirin Beer Hall (distances to hypocenter as originally reported)—X,Y,Z is sample location (cm) from building origin.*

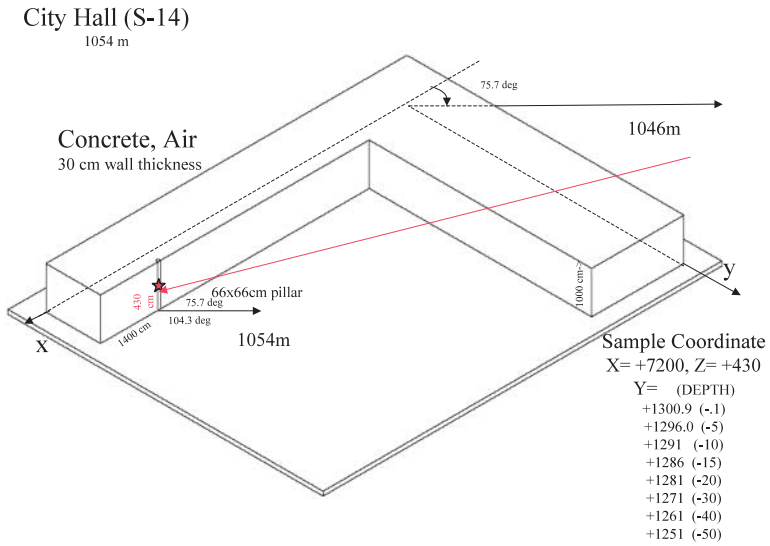

Figure A11. *City Hall Building (distances to hypocenter as originally reported)—X,Y,Z is sample location (cm) from building origin.*

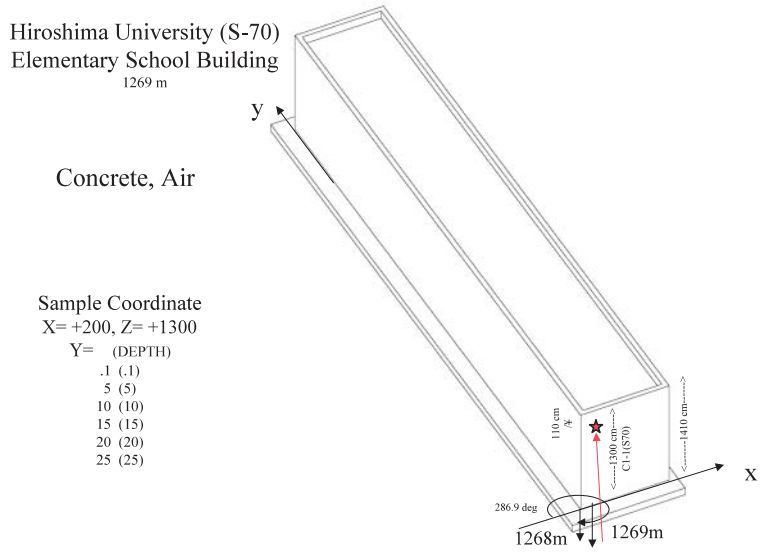

Figure A12. *Hiroshima University Elementary School Building (distances to hypocenter as originally reported)—X,Y,Z is sample location (cm) from building origin.*

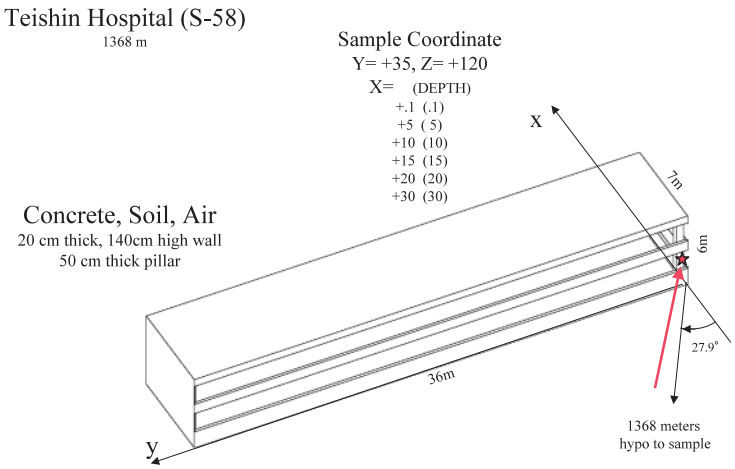

Figure A13. *Teishin Hospital (distances to hypocenter as originally reported)—X,Y,Z is sample location (cm) from building origin.*

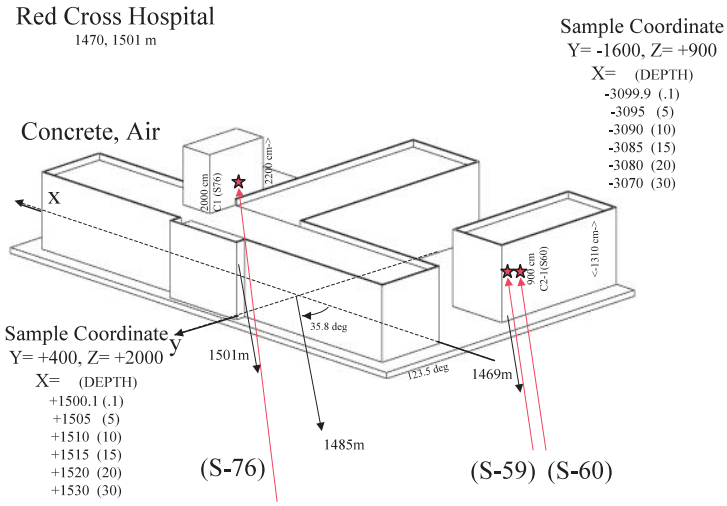

Figure A14. *Red Cross Hospital (distances to hypocenter as originally reported)—X,Y,Z is sample location (cm) from building origin.*

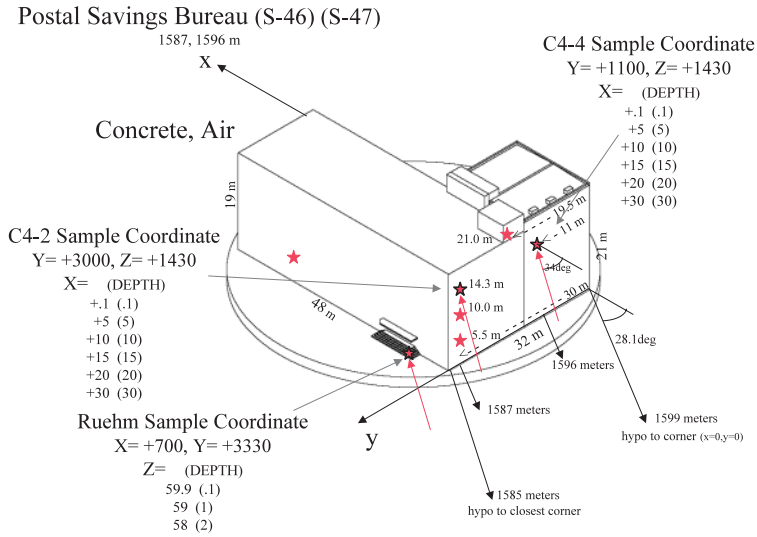

Figure A15. *Postal Savings Building (distances to hypocenter as originally reported)—X,Y,Z is sample location (cm) from building origin.*

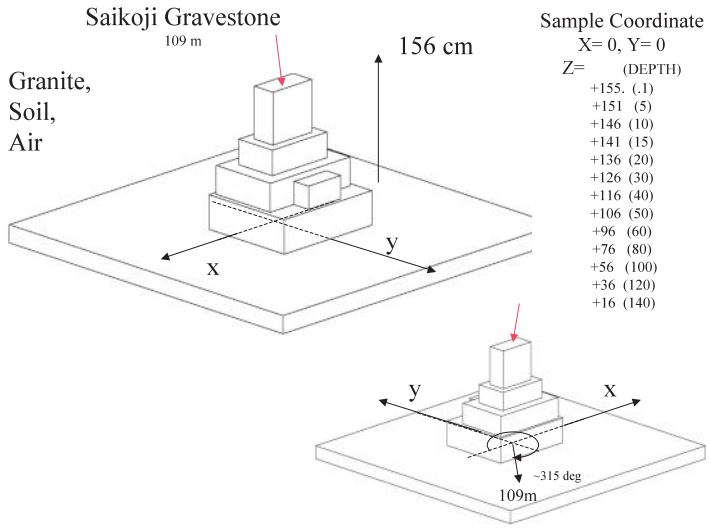

Figure A16. *Saikoji Gravestone (distances to hypocenter as originally reported)—X,Y,Z is sample location (cm) from building origin.*

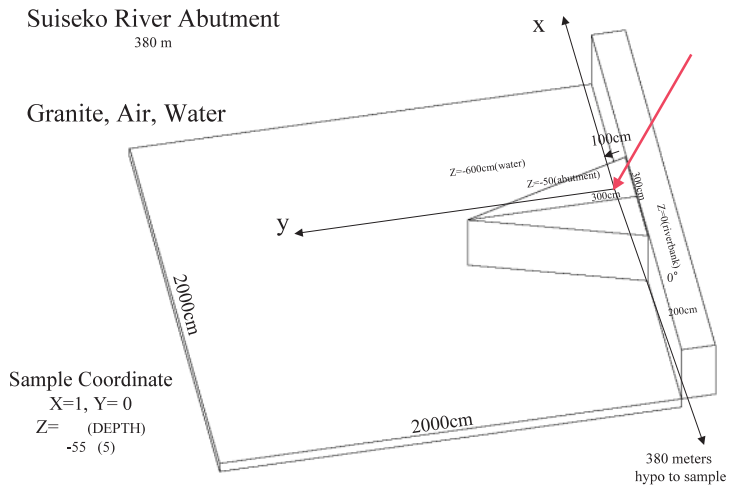

Figure A17. *Suiseko River Abutment (distances to hypocenter as originally reported)—X,Y,Z is sample location (cm) from building origin.*

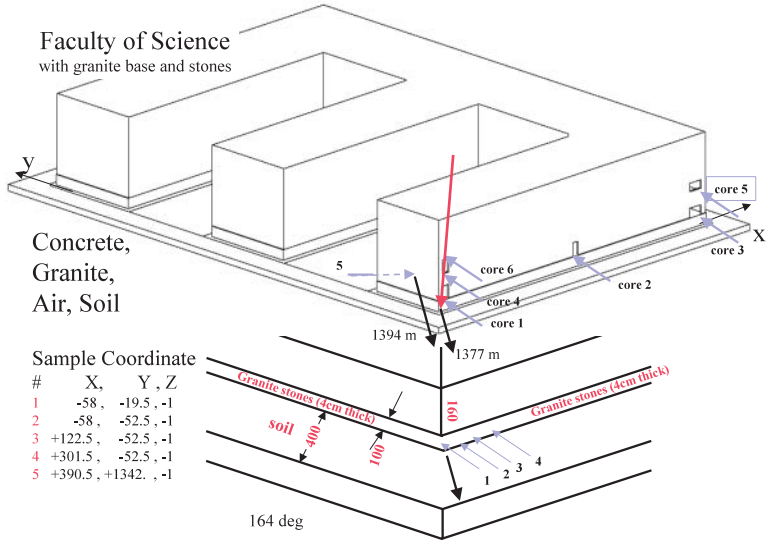

Figure A18. *Faculty of Science (distances to hypocenter as originally reported)—X,Y,Z is sample location (cm) from building origin.*

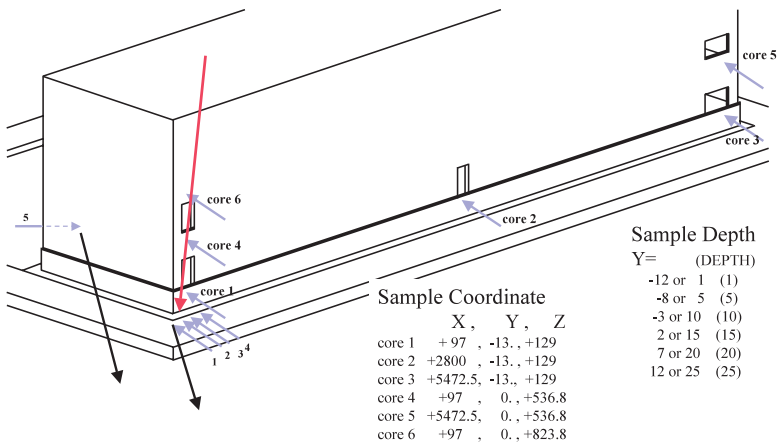

Figure A19. *Faculty of Science (distances to hypocenter as originally reported)—X,Y,Z is sample location (cm) from building origin.*

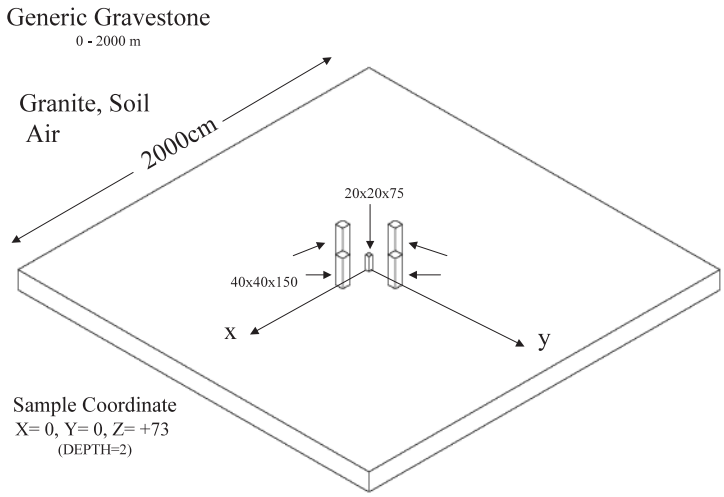

Figure A20. *Generic Gravestone (distances to hypocenter as originally reported)—X,Y,Z is sample location (cm) from building origin.*

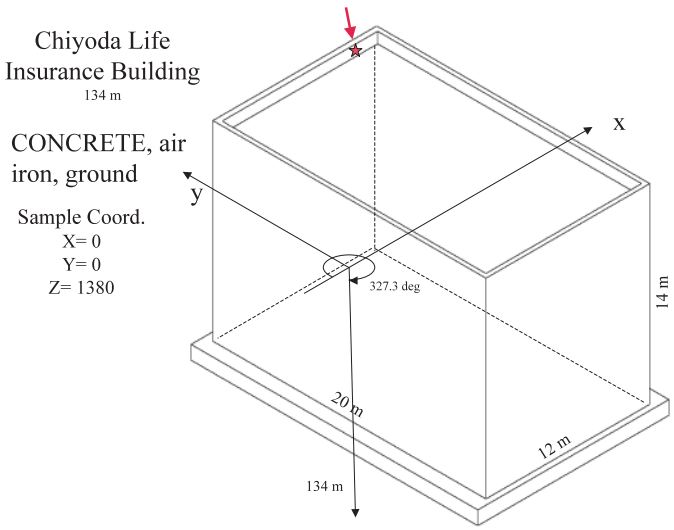

Figure A21. *Chiyoda Life Insurance Building Iron Ring (distances to hypocenter as originally reported)—X,Y,Z is sample location (cm) from building origin.*

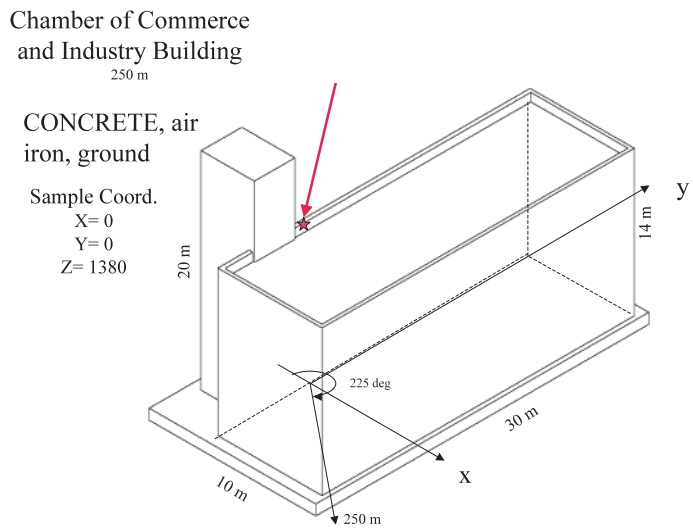

Figure A22. *Chamber of Commerce Iron Ring (distances to hypocenter as originally reported)—X,Y,Z is sample location (cm) from building origin.*

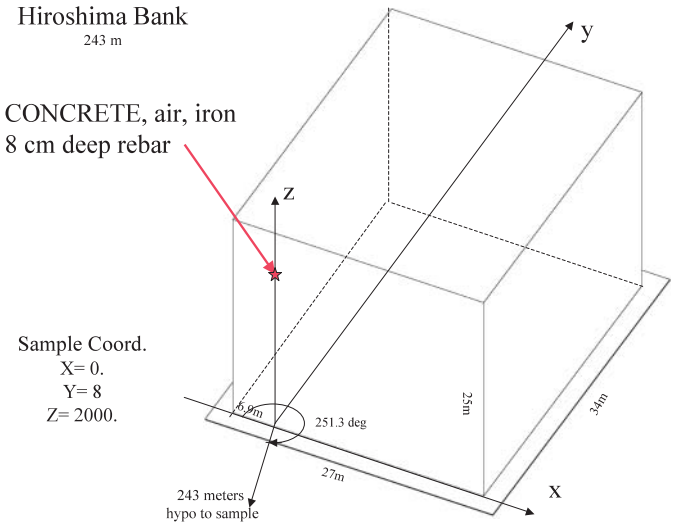

Figure A23. *Hiroshima Bank Rebar (distances to hypocenter as originally reported)—X,Y,Z is sample location (cm) from building origin.*

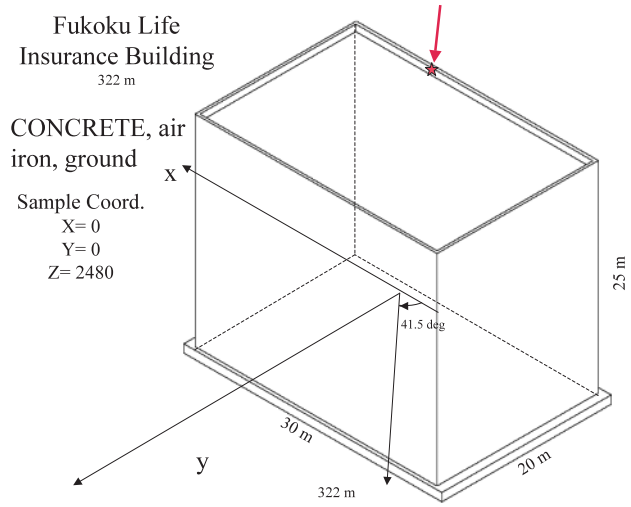

Figure A24. *Fukoku Building Iron Ring (distances to hypocenter as originally reported)—X,Y,Z is sample location (cm) from building origin.*

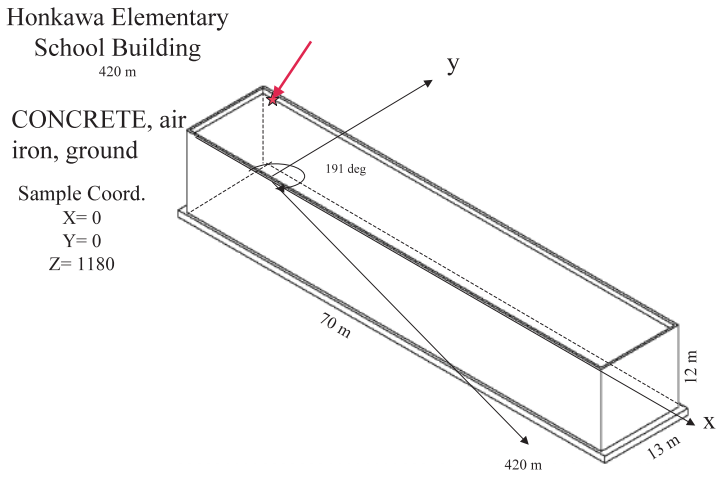

Figure A25. *Honkawa Elementary School Iron Ring (distances to hypocenter as originally reported)—X,Y,Z is sample location (cm) from building origin.*

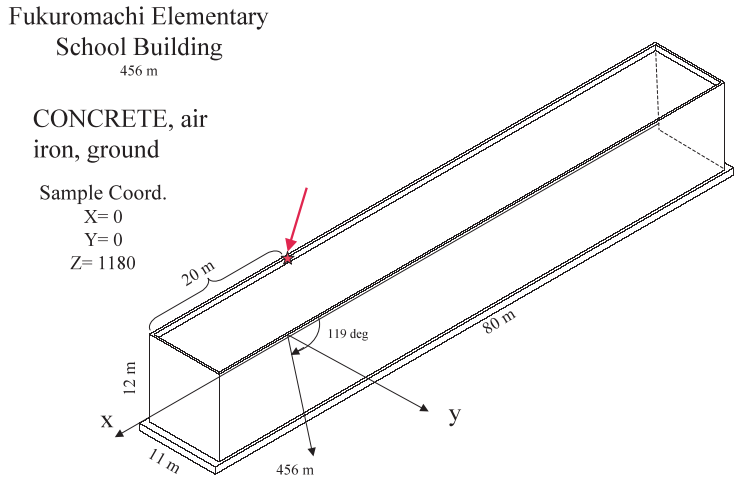

Figure A26. *Fukuromachi Elementary School Iron Ring (distances to hypocenter as originally reported)—X,Y,Z is sample location (cm) from building origin.*

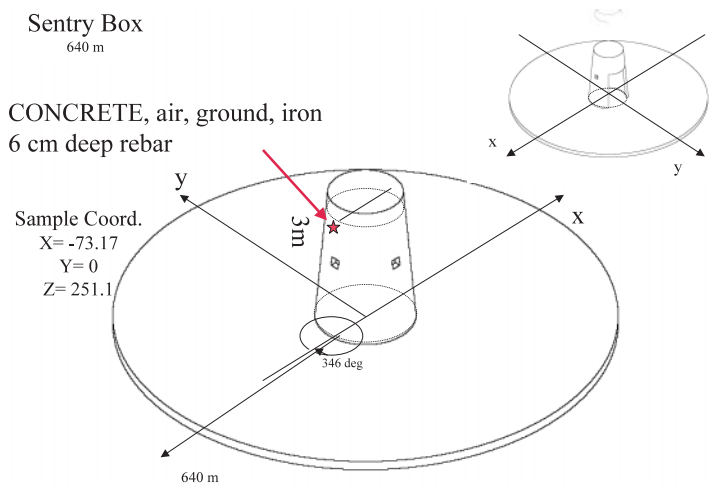

Figure A27. *Sentry Box Iron Rebar (distances to hypocenter as originally reported)—X,Y,Z is sample location (cm) from building origin.*

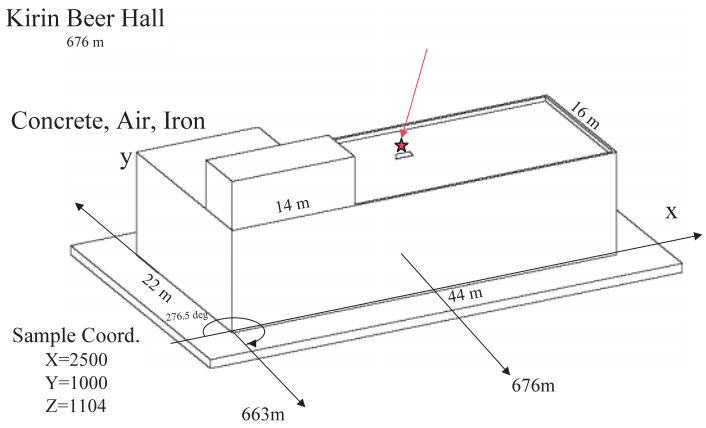

Figure A28. *Kirin Beer Hall Iron Rebar (distances to hypocenter as originally reported)—X,Y,Z is sample location (cm) from building origin.*

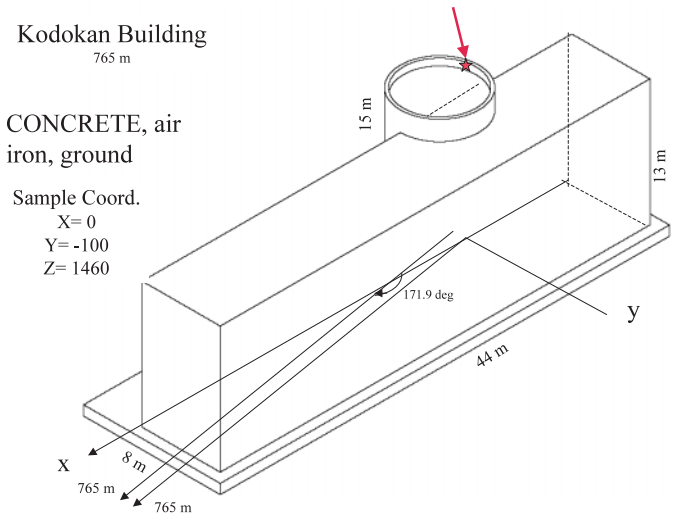

Figure A29. *Kodokan Building Iron Ring (distances to hypocenter as originally reported)—X,Y,Z is sample location (cm) from building origin.*

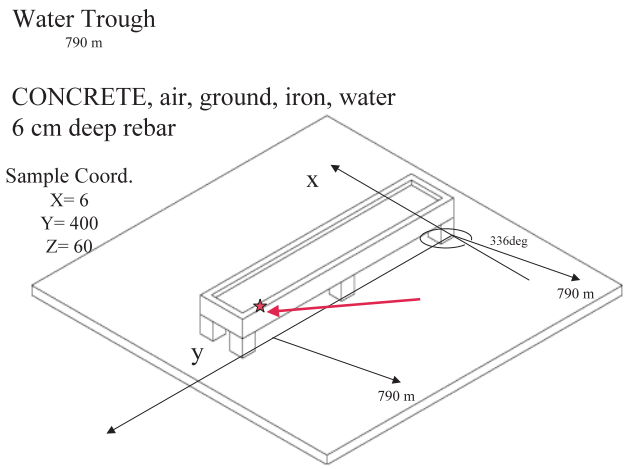

Figure A30. *Water Trough Iron Rebar (distances to hypocenter as originally reported)—X,Y,Z is sample location (cm) from building origin.*

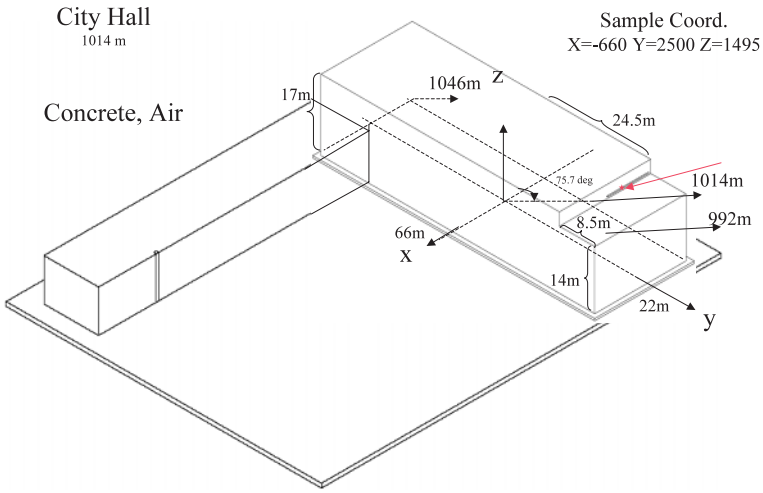

Figure A31. *City Hall Iron Railing (distances to hypocenter as originally reported)—X,Y,Z is sample location (cm) from building origin. More detailed modeling than in Figure A11 is made to account for environment of iron railing.*

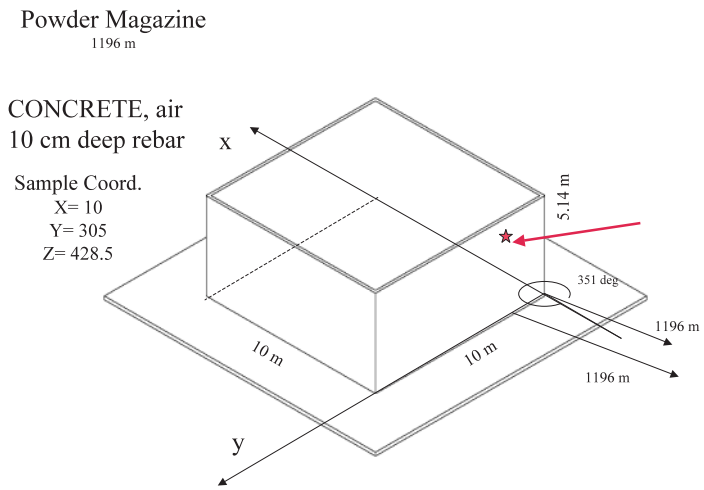

Figure A32. *Powder Magazine Iron Rebar (distances to hypocenter as originally reported)—X,Y,Z is sample location (cm) from building origin.*

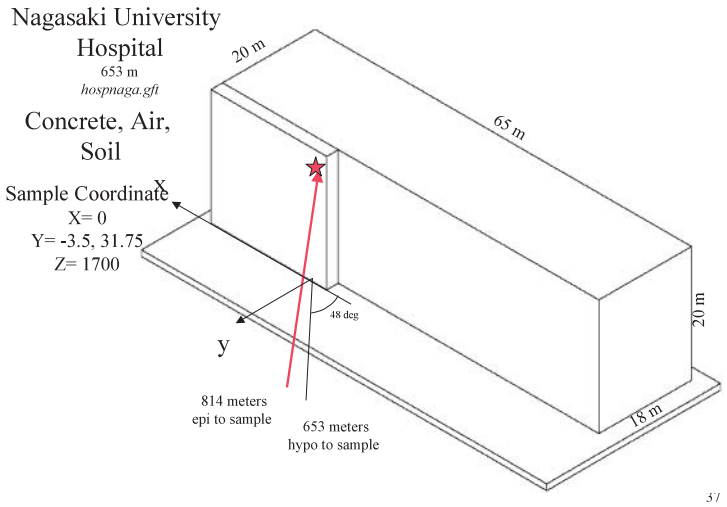

Figure A33. *Nagasaki University Hospital (distances to hypocenter as originally reported)—X,Y,Z is sample location (cm) from building origin.*

Appendix B

Calculated Thermal Neutron Transmission Factors and Resulting Sample-Specific Activation Calculations

Calculated thermal neutron transmission factors are found in Tables B1 through B5 for ^{39}K, ^{35}Cl, ^{151}Eu, ^{59}Co, ^{40}Ca, and ^{153}Eu reactions. Sample-specific activation calculations are found in Tables B6-B11 for samples measured by Nagashima et al., Ruhm et al., Straume et al. (granite), Straume et al. (concrete), Shizuma et al. (Eu) core, and Komura et al. intercomparison (Eu) samples respectively. Table B12 has calculated TFs for ^{35}Cl reactions for individual Nagasaki samples measured by Straume et al., and the resulting activation calculations are found in Table B13. More description concerning each of these tables is given in the main chapter.

Next Page